symmetry

MDPI

Article

Development of a Displacement Prediction System for Deep Excavation Using AI Technology

Chia-Feng Hsu [1,*], Chien-Yi Wu [2] and Yeou-Fong Li [3]

[1] Department of Civil Engineering, ChienKuo Technology University, Changhua City 500020, Taiwan
[2] Kenkul Corporation Company, New Taipei City 23444, Taiwan; wucy@niu.edu.tw
[3] Department of Civil Engineering, National Taipei University of Technology, Taipei 10608, Taiwan; yfli@mail.ntut.edu.tw
* Correspondence: sfhsu1013@ctu.edu.tw; Tel.: +886-958786134

Abstract: This manuscript delineates an innovative artificial intelligence-based methodology for forecasting the displacement of retaining walls due to extensive deep excavation processes. In our selection of 17 training cases, we strategically chose a wall configuration that was not influenced by the corner effects. This careful selection was conducted with the intention of ensuring that each deep excavation instance included in our study was supported symmetrically, thereby streamlining the analysis in the ensuing phases. Our proposed multilayer functional-link network demonstrates superior performance over the traditional backpropagation neural network (BPNN), excelling in the precise prediction of displacements at predetermined observation points, peak wall displacements, and their respective locations. Notably, the predictive accuracy of our advanced model surpassed that of the conventional BPNN and RIDO assessment tools by a substantial 5%. The network process model formulated through this research offers a valuable reference for future implementations in diverse geographical settings. Furthermore, by utilizing local datasets for the training, testing, and validation phases, our system ensures the effective and accurate execution of displacement predictions.

Keywords: deep excavation; artificial intelligence; wall displacement; multilayer functional-link network

Citation: Hsu, C.-F.; Wu, C.-Y.; Li, Y.-F. Development of a Displacement Prediction System for Deep Excavation Using AI Technology. *Symmetry* **2023**, *15*, 2093. https://doi.org/10.3390/sym15112093

Academic Editors: Tomasz Lewiński and Vasilis K. Oikonomou

Received: 3 October 2023
Revised: 25 October 2023
Accepted: 14 November 2023
Published: 20 November 2023

1. Introduction

1.1. Background

The complexity and data uncertainty associated with deep excavations often lead to collapse failures, which can result in damage to surrounding buildings and infrastructure. Controlling the deformation of retaining walls and preserving the stability of support systems are, thus, of paramount importance in the field of civil engineering. Numerical analysis has been widely used for predicting geotechnical engineering problems. Programs such as RIDO, TORSA, FLAC, PLAXIS, BEOO, GEO5 Sheeting check, GGU Retain, ZSOIL, GEO5 FEM, Midas GTS, and ExcWall can be used to forecast wall displacements, stress on retaining walls, preloading of support systems, and surface settlements around excavations. Deep excavation involves complex soil–structure interactions, which can be simplified using one-dimensional elastic beam theory or two- and even three-dimensional finite-element analysis. The finite-element method is widely used in geotechnical engineering, structural analysis, and materials science, with numerous research papers and engineering case studies validating the efficacy of these methods.

Geotechnical engineering involves highly complex interactions among soil parameters and environmental factors. Regardless of the analysis program, the selection of parameters is crucial to the precision and accuracy of wall displacement predictions. This has prompted research into the use of artificial intelligence to deal with the engineering issues related to excavation wall displacements. Artificial intelligence utilizes mathematical models to conduct analysis based on accumulated experience or data, allowing it to learn and extract

knowledge automatically via learning algorithms. The objective of this study was to utilize a neural network to develop an improved model for the prediction of wall displacements prior to excavation.

1.2. The Literature Review

- Factors affecting retaining wall deformation in deep excavation

The deformation of the retaining wall is influenced by the mechanical properties of soil and ground subsidence and other factors. Numerical analyses and case studies indicate that a large number of factors can affect wall deformation [1–15]. The following studies have investigated the factors influencing excavation integrity:

In 1972, Palmer and Kenney [1] used finite-element analysis to identify six parameters affecting support excavation behavior. These parameters were (1) soil elastic modulus, (2) soil shear strength, (3) in situ initial stress, (4) friction force between soil and retaining wall, (5) retaining wall stiffness, and (6) support stiffness;

In 1981, Mana and Clough [2] used finite-element analysis and case studies to identify five factors affecting deep excavation behavior. These factors were (1) safety factor to prevent heaving (related to the penetration depth of the wall and soil strength), (2) soil strength, (3) safety stiffness of the support system (associated with the stiffness of the wall and support), (4) pre-stress applied to the support, and (5) geometry of the excavation face;

In 1981, O'Rourke [3] reported that pre-construction operations and construction methods could affect ground deformation, claiming that lateral displacements in retaining walls could be attributed to differences in the excavation procedures used in forward and reverse construction methods;

In 1987, Chen [4] listed six factors that could affect deep excavation ground deformation. These parameters were (1) size (area) and depth of the excavation scope, (2) type of soil, (3) type of retaining system, (4) excavation procedure, installation of retaining systems, and worker skill level, (5) duration for which the excavation face is left open, and (6) groundwater removal;

In 1989, Wong and Broms [5] used finite-element analysis to identify five factors affecting deep excavation variables, such as the undrained shear strength, the width and depth of excavation, the wall stiffness, the penetration depth, and the depth of the hard stratum beneath the bottom of the excavation;

In 1990, Clough and O'Rourke [6] used case studies to illustrate the movement of retaining walls due to excavation, resulting in the identification of eight influential factors. These factors were (1) soil conditions, (2) groundwater level conditions, (3) variations in groundwater level, (4) depth and shape of the excavation site, (5) stiffness, support, and types of retaining walls, (6) construction methods of retaining walls, (7) equipment and overloading conditions surrounding the excavation, and (8) exposure duration of retaining walls during excavation;

In 1992, Hu [7] identified 17 factors affecting deep excavation deformation and classified them into three categories, as listed below:

I. Inherent conditions: soil layer characteristics; groundwater pressure distribution; environmental conditions of the excavation area; surrounding buildings and traffic conditions;
II. Design conditions: geometry of the excavation area; excavation depth; retaining structures; support systems; support pre-stress; excavation procedures and methods at various stages; methods for constructing permanent structures;
III. Construction conditions: construction sequence and dewatering control; water tightness of retaining walls; timing and control of excavation; timing of applying pre-stress; construction techniques of the support structure system timing of support removal;

In 1993, Lin and Lee [8] identified seven factors affecting deep excavation deformation. These factors were (1) lateral deformation of retaining walls, (2) construction dewatering, (3) retaining wall construction, (4) leakage or sand egress at the seams of retaining walls during dewatering, (5) heaving, (6) removal of retaining walls or old foundations, and (7) creep behavior of soil;

In 1994, Masuda at el. [9] examined 52 case studies of deep excavation ground deformation. They listed 11 factors divided into two categories, as listed below:

I. Soil stiffness: type of soil in the excavation area; properties of soil in the excavation area (such as undrained shear strength, elastic modulus, etc.); ground improvement measures; and groundwater conditions;
II. Construction conditions: stiffness of the retaining wall; spacing and quantity of supports; pre-stress in supports; excavation methods (such as top–down or bottom–up methods); length of the retaining wall; scale of excavation (such as depth and width of excavation); and other construction conditions;

In 1998, Lao and Zheng [10] examined disaster cases involving wall deformation. They listed ten influential factors, as listed below: (1) soil type in the excavation area; (2) retaining wall stiffness; (3) support system integrity; (4) construction dewatering; (5) safety factor against heave; (6) uplift and sand boiling; (7) construction load configuration; (8) excavation elevation; (9) worksite layout; and (10) excavation method;

In 2000, Lee et al. [11] examined disasters related to deep excavation to find four influential factors. These factors were (1) retaining wall failure, (2) heave failure at the excavation face, (3) leakage pipe erosion failure in the retaining wall, and (4) sand boiling failure at the excavation face;

In 2002, Ou [12] categorized eight factors affecting wall deformation. These factors were (1) safety factor for stability, (2) excavation face width, (3) excavation depth, (4) penetration depth of the retaining wall, (5) stiffness of the retaining wall, (6) support stiffness, (7) support spacing, and (8) support pre-stress;

In 2017, Goh et al. [13] used the hardening soil model to investigate the influences of soil properties, wall stiffness, excavation length, excavation depth, and clay thickness at the base of the excavation and wall embedment depth on the maximum wall deflection induced by braced excavation;

In 2020, Zhang et al. [14] conducted a finite-element analysis considering the anisotropy of undrained shear strength to examine the impact of total stress-based anisotropic model NGI-ADP parameters on the base stability of deep-braced excavations in clays;

In 2021, Zhang et al. [15] conducted a case study involving a deep foundation pit project adjacent to the shield tunnel of Hangzhou Metro Line 2. They analyzed the changes in confining pressure distribution around the neighboring shield tunnel caused by the excavation of the foundation pit. Additionally, they developed a simplified finite-element model to calculate the internal forces acting on the segment ring structure.

The results of these studies are integrated in Table 1, where the factors affecting wall deformation can be broadly classified into five categories: environmental; planning and design; construction; time; and other. Among construction factors, some are not inherent to the activity but rather to quality control. In the current study, we focused exclusively on factors associated with construction methods. The other category includes heavy rainfall and a corresponding rapid increase in groundwater level, which can affect the mechanical properties of the soil and affect the equilibrium relationship. It also includes repeated loading from earthquakes, which can cause soil liquefaction and the loosening of support systems [16].

Table 1. The literature review of the factors affecting retaining wall deformation.

Influence Type	Influence Condition	Influence Factor
I	Environmental	1. Type and properties of excavation soil; 2. Distribution of groundwater pressure; 3. Configuration of construction loads; 4. Surrounding buildings and traffic conditions.
II	Design and Planning	1. Excavation face geometry; 2. Excavation depth; 3. Ground improvement (Yes/No); 4. Stiffness of retaining structure; 5. Penetration depth of retaining wall; 6. Support system (stiffness and spacing); 7. Preloading of support system; 8. Excavation sequence and construction method for each stage; 9. Construction method for permanent structures.
III	Construction	1. Construction sequence and dewatering control; 2. Water tightness of retaining wall; 3. Timing and control of excavation; 4. Timing of applying preload; 5. Timing of support installation and removal and construction techniques.
IV	Time	1. Duration of excavation face exposure; 2. Soil creep behavior.
V	Other	1. Heavy rainfall; 2. Earthquake.

- Research Materials

Ou [12] has classified deformation characteristics due to excavation into 11 categories. Clough and O'Rourke [6] identified three types of deformation (shapes) pertaining to retaining walls, including cantilever displacement, deep-seated inward displacement, and the combination of the cantilever and deep-seated inward displacements. Note that deep excavation initially induces cantilever displacement followed by deep-seated inward displacement. Thus, most of the deformations observed following the completion of an excavation fall into the category of combined displacement [17].

Based on field observation data from numerous deep excavation projects in the Taipei Basin, Ou et al. [18] reported that the maximum lateral displacement of the retaining wall generally occurred near the final excavation level. The one exception is the occurrence of maximum displacement at the top due to cantilever displacement in the initial stage of excavation. Based on monitoring data from Taipei Metro projects, Wu et al. [19] categorized the deformation curves of diaphragm walls into four types: standard; rotational; multiple fold; and cantilever;

- Effects of contemporary wall design

1. Relationship between penetration depth and excavation depth

Penetration depth refers to the depth at which a diaphragm wall penetrates the soil layer, which is calculated by subtracting the final excavation depth from the total length of the wall. Insufficient penetration depth can result in heaving and squeezing. Our analysis of previous work on penetration depth and excavation depth revealed that the D/Hf values obtained from the Taipei Basin were higher than those from the Kaohsiung area [20–23]. This can be explained by the distribution of weak clay layers, which is wider in the Taipei Basin than in the Kaohsiung area. In the design of retaining structures in weak clay layers,

it is often advantageous to increase the penetration depth of a wall to minimize the risk of heaving and squeezing;

2. Relationship between maximum wall displacement and excavation depth

Some research revealed that when using bottom–up construction, the maximum wall deformation ranges from 0.05% to 0.64% of the excavation depth, with an average of 0.35% [18,20–24]. Under top–down construction, the maximum wall deformation ranges from 0.12% to 0.62% of the excavation depth, with an average of 0.37%. The average wall deformation is 0.36%;

- Predicting wall displacement of the deep excavation

Methods used in the analysis of deep excavation can be divided into six categories: (1) assumed fixed-point; (2) elastic; (3) elastic–plastic; (4) plastic; (5) stress superposition; and (6) finite-element [25]. Most of these methods were initially performed on paper; however, manual calculations have gradually been replaced by software solutions. The computational methods most commonly used for deep excavation analysis are the finite-element and elastic–plastic methods. In Taiwan, the one-dimensional RIDO and TORSA 2.0 version programs are popular software tools for excavation prediction analysis;

- RIDO

The software program RIDO 3.07 version was developed by the French company Robert Fages Logiciels in 1983. Based on the Winkler model and the theory of elastic–plastic equilibrium, RIDO simulates the bending moment, shears, deformations, and support loads experienced by retaining walls during various stages of excavation. That model considers soil properties, wall stiffness, groundwater level changes, construction procedures, support systems during the construction process, and preloading [26]; It is widely used in Taiwan for the simulation of deep excavation projects, and has been shown to generate reasonable soil parameter values [27–31].

- Artificial neural network

Researchers have been developing neural networks since 1957. At present, there are 11 network models of four types. The most common approach to the prediction of excavation-related wall displacements involves supervised learning models. Backpropagation neural networks (BPNN) have proven highly effective in these prediction scenarios, as evidenced by a success rate from 77% to 83% [32,33]. Huang [26] studied ten cases of inverse construction using a relatively complete database of the Taipei Basin. The relative errors between the predicted maximum displacement and the actual maximum displacement location accounted for over 85%, representing good prediction capability. Lin [16] achieved good results in predicting wall displacements using evolutionary fuzzy neural networks. Li [34] achieved similar results using an evolutionary support vector machine inference system. By using the multilayer functional-link network (MFLN) prediction model, Wu and Chen [35] achieved an average prediction error for the maximum wall displacement in each excavation stage of 9.2%, far exceeding the results obtained using a backpropagation neural network (13.1%) or the RIDO program (22.7%).

2. Methodology

The behavior of retaining wall deformation and its impact on the surrounding ground surface in the context of deep excavation have been studied extensively. Note that when using the finite-element method, accuracy in assessing wall deformation and surface settlement relies on soil parameter values obtained from laboratory tests. Unfortunately, the values obtained via laboratory testing seldom match the conditions at the construction site. Numerous researchers have used feedback analysis for calibration in an effort to mitigate the effects of soil parameters and construction activity [36–40], and the combined use of the finite-element method with feedback analysis has proven somewhat effective in simulating deformations. However, feedback analysis is limited by the selected soil parameters and

soil models [41]. This has prompted the adoption of artificially intelligent methods to deal with engineering problems related to excavation-induced wall displacements [16,41,42].

In neural networks, there is no need to explicitly define the mathematical relationships among variables, as they can be learned from examples and feedback. In the current study, we used a modified multilayer functional-link network (MFLN) model to enhance accuracy in the prediction of retaining wall displacements under non-excavated conditions. The model was trained and evaluated using data from 17 case studies, which included 2475 examples for learning and 141 examples for testing.

Neural Networks

As shown in Figure 1, neural networks comprise artificial neurons, which process input signals and then output the results to other processing units. The relationship between the input and output values of a given processing unit (neuron) in a neural network can be represented by a weighted sum of the input values, followed by the application of an activation function [43].

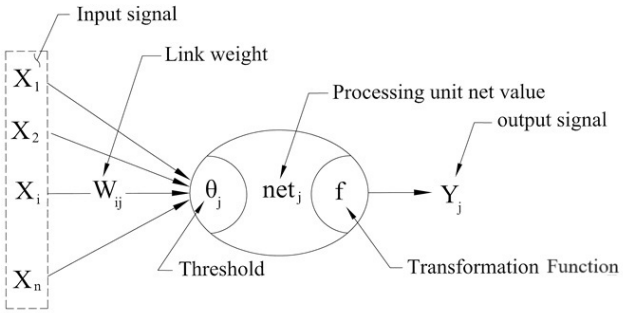

Figure 1. Artificial neural network model (Referenced and redrawn from Yeh [43]).

where

Y_j = Output signal (output), mimicking the output signal of a biological neuron.

f = Transfer function, which is a mathematical formula used to transform the weighted sum of input values from other processing units into the output value of the processing unit.

W_{ij} = Connection weight (weight), mimicking the synaptic strength of a biological neuron.

X_i = Input value (input), mimicking the input signal of a biological neuron.

θ_j = Threshold.

- Neural networks perform two main processes:
  1. Learning: The network acquires knowledge via a learning algorithm, which iteratively refines the weights of its connections. Learning algorithms fall into three primary categories: supervised learning; unsupervised learning; and associative learning. Each algorithm is based on an energy function, which serves as a metric for evaluating the learning performance of the network. The learning process is essentially a process of minimizing the energy function;
  2. Recall: The network employs a recall algorithm to process input data and generate an output.

(1) Backpropagation neural network

The most common learning model is the backpropagation neural network (BPNN), which leverages the gradient descent method to iteratively minimize the error function with the aim of minimizing the disparity between the desired target output values and predicted output values generated by output units. The BPNN architecture comprises the following three levels shown in Figure 2, including the input layer, hidden layer, and output layer.

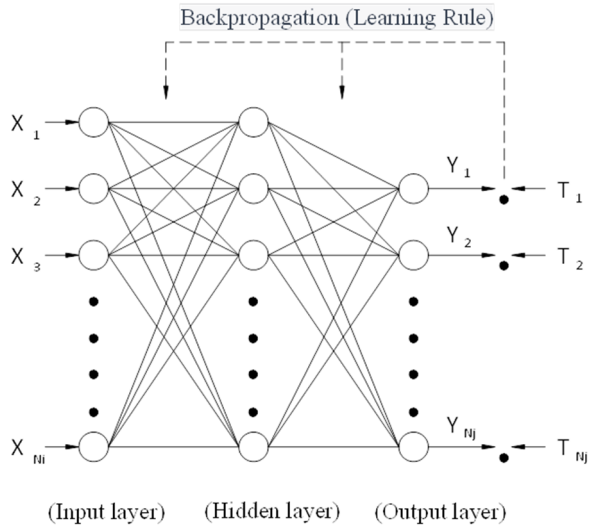

Figure 2. Backpropagation neural network architecture diagram.

where

X_n: Input variable.

Y_n: Output variable.

T_n: Expected inference value.

BPNNs enable high learning accuracy and fast recall speeds; however, they are affected by an inefficient learning design and the risk of converging to local minima;

(2) Multilayer functional-link network (MFLN)

The MFLN was adopted in this study, which is essentially a BPNN network with "logarithmic" and "exponential" input and output units in the input and output layers (as shown in Figure 3) [43]. The network learning algorithm also uses the "Generalized Delta Rule" to enhance learning capabilities.

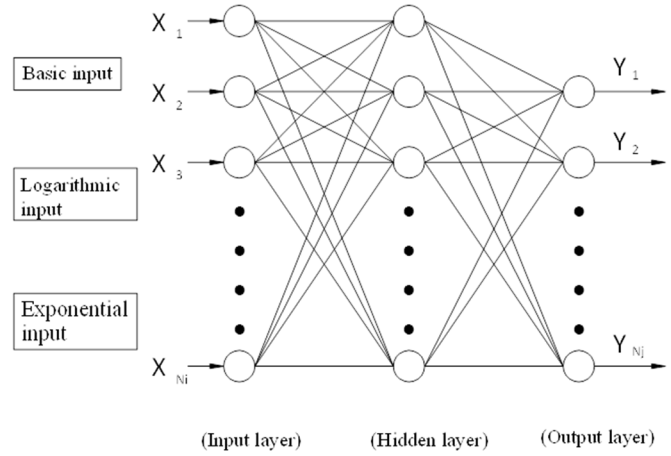

Figure 3. A schematic diagram of a multilayer feedforward neural network architecture.

The MFLN utilizes hidden units to transform independent variables received from the input units and transformed variables provided by the logarithmic and exponential input units into nonlinear functions, which are organized into a nonlinear function at the output units. This design overcomes many of the drawbacks of backpropagation networks, such as insufficient hidden units and an extended learning process for highly nonlinear problems.

The key difference between backpropagation networks and the MFLN is the fact that the former uses one regular neuron to represent a variable, while the latter uses three neurons (regular, logarithmic, and exponential neurons) to represent a variable. The

sensitivity of the logarithmic neuron to the lower value range of the variable and the sensitivity of the exponential neuron to the higher value range enhance the accuracy of the MFLN. Note that the logarithmic and exponential neurons can be considered hidden processing units located in the input layer.

3. Case Analysis and Prediction Model Development

This study collected data from 17 deep excavation sites in the Taipei Basin (Wu and Chen [44]). We considered each excavation stage as an independent case, which resulted in a database of 82 stages. All of these cases involved continuous underground walls constructed using top–down excavation methods. Supplementary Table S1 lists the basic information of the cases, and Figure 4 presents a map showing the spatial distribution of the sites. From among these 17 cases, we selected one monitoring point (on a wall unaffected by corner effects; the purpose of this was to ensure that the chosen deep excavation cases all featured symmetrical supports and wall bodies, facilitating simplified half-type analysis in subsequent stages) for training the neural network. From among the cases with relatively complete data, we selected another monitoring point on a wall as a reference for subsequent simulations and predictions. Table S2 lists basic information on the monitoring points;

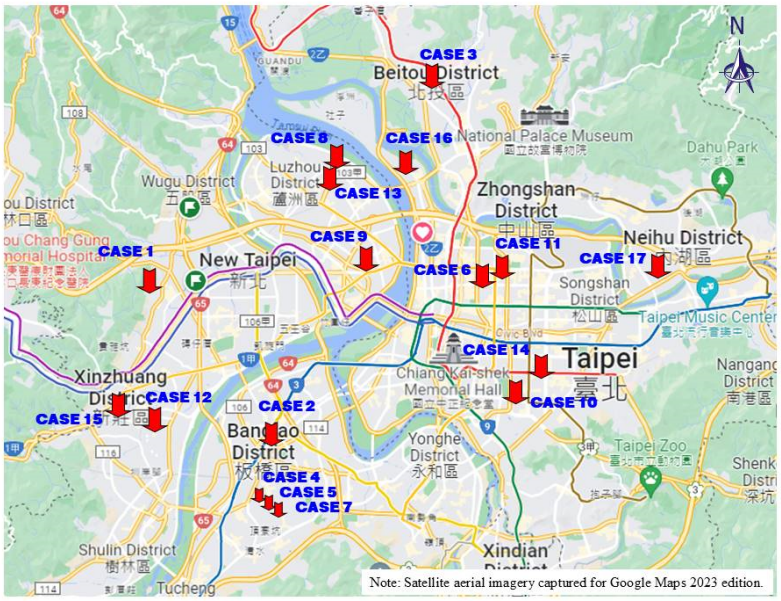

Figure 4. A schematic diagram illustrating the distribution of the cases in Taipei basin.

- Network Construction

The flowchart for the prediction model established in this study is as follows in Figure 5:

Ji et al. [33] reported that wall deformation behavior following the initial excavation stage is of the cantilever type; however, the observed phenomena are greatly influenced by unknown factors, such as environmental and material stress properties. Note that displacements occurring during the second stage of excavation are influenced by deformations accumulated in the previous stage. Taken together, we concluded that displacement data from Stage 1 and Stage 2 were of limited value for training, testing, and validating the neural network. We, therefore, excluded 34 of the 82 stages, which left 48 stages for training and testing. Note that in training and testing the neural network, the displacement data at each observation point were treated as an individual data point, which resulted in 2475 records for training and 141 records for testing.

As mentioned in the previous section, the deformation of deep excavation walls can be affected by a wide range of factors. The inclusion of all possible factors would result in a prediction network that is too complex for practical applications. Thus, we selected

a subset of key influential factors based on our literature review and the experience of the authors [16,26,33]. The proposed network comprised a total of 12 input variables; the definitions are shown in Figure 6.

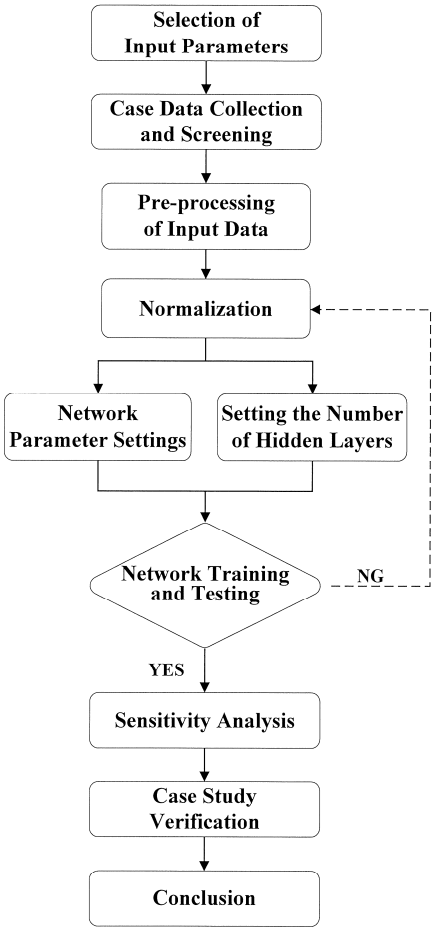

Figure 5. Flowchart of the Prediction Model Establishment.

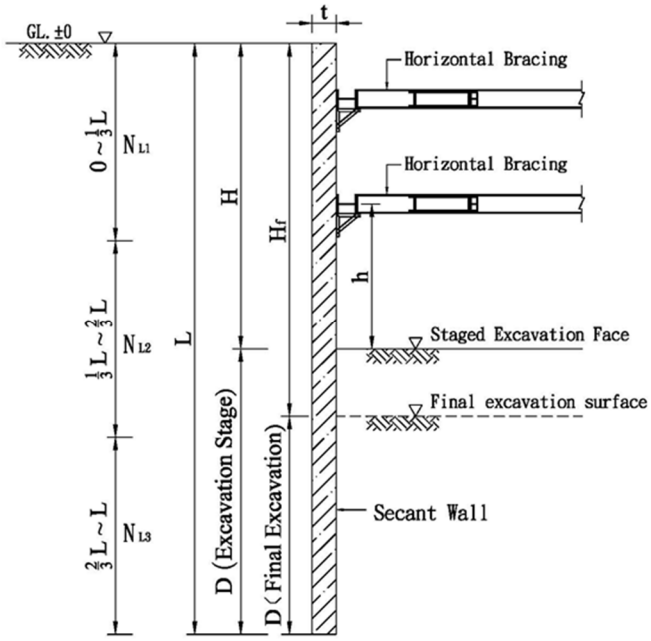

Figure 6. A schematic diagram illustrating the definition of input variables.

1. Depth ratio of penetration to final excavation depth (D/H_f);
2. Depth ratio of penetration to excavation depth (D/H);
3. Excavation depth (H);
4. Wall thickness (t);
5. Distance from support to excavation face (h);
6. Soil *SPT-N* values (NL_i, i = 1~3);
7. Wall displacement at the previous stage for observed point (Δ_i, i = 1~3);
8. Depth of observation point (R).

Note that the 12 variables include three related to soil properties (NL_i), which represent the equivalent *SPT-N* values of the soil in the following ranges: N_{L1} (from 0 to 1/3L); N_{L2} (from 1/3L to 2/3L); and N_{L3} (from 2/3L to L), where L indicates the depth of the wall. The 12 variables also include three related to accumulated wall displacement (Δi) at a given monitoring point in the three previous stages (i = 1~3). For example, in the prediction of Stage-5 displacements, input variable Δ_1 corresponds to that point in Stage 4; Δ_2 corresponds to that point in Stage 3, and Δ_3 corresponds to that point in Stage 2. The output variable is the predicted horizontal displacement at a specific observation point.

3.1. Establishing an Optimal Model

The 12 input variables were assembled into six network model combinations for use in training and testing the BPNN and MFLN. The training and testing results were then used to elucidate the effects of each input variable on the network with the aim of identifying those that should be included in the final network (as shown in Table 2). To ensure comparability, we employed consistent learning parameters, including the number of hidden layers, the number of hidden layer nodes, the number of learning iterations, the learning rate, and the inertia.

Table 2. List of input variable combinations.

Network Architecture	Input Variable	Number of Variable
B-1	D/H, H, t, h, N_{L1}, N_{L2}, N_{L3}, Δ_1, Δ_2, Δ_3, R	11
B-2	D/H_f, H, t, h, N_{L1}, N_{L2}, N_{L3}, Δ_1, Δ_2, Δ_3, R	11
B-3	D/H, H, t, h, N_{L1}, N_{L2}, N_{L3}, R	8
B-4	D/H, H, t, h, Δ_1, Δ_2, Δ_3, R	8
B-5	D/H, H, t, h, R	5
B-6	D/H_f, H, t, h, R	5

Table 3 summarizes the errors obtained using the various networks. Learning performance is indicated by the root mean square error (RMSE), where a smaller value indicates superior learning performance. Table 4 lists the sensitivity of each input variable to the output variable, where a positive higher value indicates a stronger positive correlation, whereas a higher negative value indicates a stronger negative correlation.

Table 3. Training and testing results of the BPNN and MFLN.

Network Architecture	BPNN				MFLN			
	Training RMS	Testing RMS	Coef.	RMSE	Training RMS	Testing RMS	Coef.	RMSE
B-1	0.0236	0.0262	0.9005	0.2281	0.0139	0.0240	0.8976	0.2092
B-2	0.0237	0.0311	0.8441	0.2710	0.0136	0.0259	0.8923	0.2255
B-3	0.0328	0.0263	0.8576	0.2293	0.0184	0.0303	0.7997	0.2646
B-4	0.0288	00272	0.8936	0.2371	0.0195	0.0311	0.8973	0.2707
B-5	0.0613	0.0442	0.8698	0.3858	0.0345	0.0365	0.7589	0.3184
B-6	0.0487	0.0611	0.8369	0.5330	0.0317	0.0251	0.9118	0.2187

Table 4. Sensitivity analysis summary table for the network.

Input Variable Item		*D/H*	*H*	*t*	*h*	N_{L1}	N_{L2}	N_{L3}	$\triangle_1$	$\triangle_2$	$\triangle_3$	*R*
BPN	Ranking	2	10	9	4	5	8	3	1	11	7	6
	Sensitivity value	0.67	−1.474	−1.107	0.11	−0.066	−0.94	0.31	4.57	−2.098	−0.218	−0.183
MLFN	Ranking	7	8	5	10	11	1	2	4	6	9	3
	Sensitivity value	−0.325	−0.354	−0.2	−0.404	−0.578	0.05	0.00	−0.183	−0.315	−0.375	−0.034

Model B-1 outperformed the other models in terms of training and testing performance, as evidenced by the RMSE and sensitivity results. We, therefore, selected the input variables used in the B-1 network model as input variables for the network proposed in this study.

From the literature reviews, six network configuration parameters can significantly affect training and testing results; those six parameters are the number of units in the first hidden layer, the number of logarithmic processing units, the number of exponential processing units, the number of learning cycles, the learning rate, and the inertia factor. In this study, the optimal values for these six parameters were obtained via trial and error. The optimization network training process is shown in Figure 7 and Table A1, and the results are summarized in Appendix A (Table A2). The optimal parameter values were used to establish new network models for training and testing, after which the network output values were rescaled to obtain test values (predictions). The predicted values were compared with values obtained via on-site monitoring to create the prediction vs. monitoring displacement maps for each stage of the excavation process (shown in Appendix B, Figures A1–A3). In comparing the performance of the two networks, the preliminary evaluation criterion was prediction accuracy for the maximum displacement and the depth of maximum displacement after each stage of the excavation. Note that these indicators are of particular interest to construction managers.

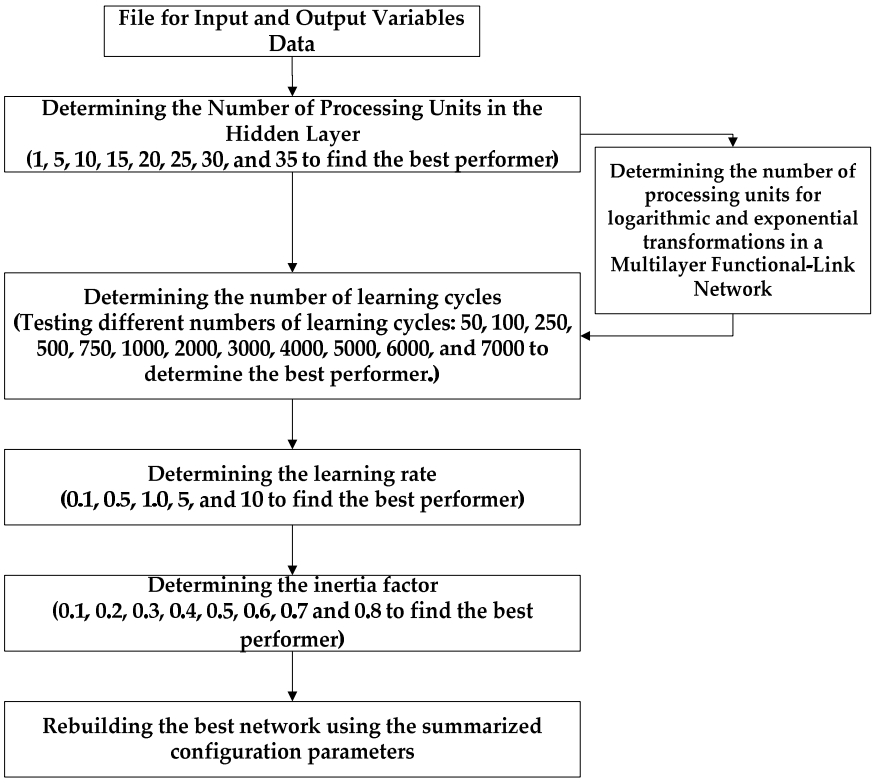

Figure 7. Flowchart of the best network training process.

The relative errors between actual and predicted maximum displacements were calculated for each stage, the results of which are summarized in Table 5. In terms of maximum displacement error, the MFLN outperformed the BPNN, except in the third-stage excavation, in which the error of MFLN (24.4%) significantly exceeded that of the BPNN (10.6%). In terms of maximum displacement location, the predictions of the MFLN and BPNN were close to the actual values in the first two stages; however, the predictions of the MFLN for the third-stage excavation had a significantly larger error (nine nodes compared to the five nodes of the BPNN, where each node represented a 0.5 m interval).

Table 5. The comparison of the monitoring and predicted displacements.

	Monitoring Value		BPNN				MFLN			
	Max. Displacement (cm)	Occurrence Location (m)	Max. Predicted Displacement (cm)	Error (%)	Occurrence Location (m)	Error (%)	Max. Predicted Displacement (cm)	Error (%)	Occurrence Location (m)	Error (%)
The 3rd-stage excavation	0.19	−13.81	0.21	10.6%	−11.31	−2.50	0.24	24.4%	−9.31	−4.50
The 4th-stage excavation	0.89	−11.81	0.69	22.5%	−12.31	0.50	0.75	15.7%	−12.81	1.00
The 5th-stage excavation	1.4	−13.31	1.09	22.1%	−13.31	0.00	1.38	1.5%	−13.31	0.00

3.2. Criteria Used in Evaluating Prediction Performance

This study adopted the evaluation criteria proposed by previous scholars to assess the accuracy of the proposed system in the prediction of wall displacements. Note that the standards were adjusted according to the objectives of this study. The evaluation criteria and standards are outlined below:

1. Displacement at each monitoring point:

Performance in predicting wall displacement at each monitoring point was assessed in terms of relative error, as follows: (1) successful (relative error = 0–20%); (2) acceptable (relative error = 20–30%); (3) poor (relative error = 30–40%); and (4) failure (relative error $\geq$ 40%);

2. Maximum wall displacement in each stage of excavation:

Performance in predicting maximum displacement in each stage of excavation was assessed in terms of relative error, as follows: (1) excellent (relative error = 0–10%); (2) poor (relative error = 10–20%); and (3) unacceptable (relative error $\geq$ 20%);

3. Location of maximum wall displacement:

Performance in predicting the location of maximum wall displacement was assessed in terms of deviation from actual values, as follows: (1) successful (0–2 m); (2) acceptable (2–4 m); (3) poor (4–6 m); and (4) failure (>6 m).

3.3. Case Study Verification

The predictive capability of the optimal network was assessed using validation data from a monitoring pipe (Case No. 15, Monitoring Pipe SI-03) that were not included in the training or testing datasets. From the displacement data, we derived 168 validation data points. The predictive accuracy of the BPNN and MFLN were compared with that of RIDO. Note that when using RIDO, the selection of geological parameters is crucial. In the current study, we adopted the soil parameters recommended by Chen and Ji [45], as follows: clay (0.3; from 50 m^{-1} to 200 m^{-1}); and sand (50 t/m^3 to 200 t/m^3).

Out of the 168 available observed displacements for validation, the predicted and monitored displacement maps were created for each excavation stage, as shown in Figures A4–A6. Additionally, the level statistics for each observation point in each excavation stage were summarized in Tables A3–A5. It can be seen that the MFLN network achieved a success rate of approximately 67.9% in the third excavation stage, 51.8% in the fourth excavation stage, and 91.1% in the fifth excavation stage. Comparatively, the BPNN achieved a success rate

of approximately 58.9% in the third excavation stage, 42.9% in the fourth excavation stage, and 82.1% in the fifth excavation stage. These results indicate that the MFLN network can improve the accuracy of wall displacement prediction. Furthermore, from the displacement maps, it can be observed that both the BPNN and MFLN networks outperformed the RIDO program in terms of predictive capability.

Table 6 lists the predicted maximum displacements and corresponding level classifications for each stage of the excavation. The performance of the MFLN in predicting wall displacements was assessed in terms of relative error; the results are as follows: the third-stage excavation and the fourth-stage excavation (10%; excellent); the fifth-stage excavation (14.6%; poor). The performance of the BPNN in predicting wall displacements was as follows: the third-stage excavation (7%; excellent). The performance of RIDO in predicting wall displacements was as follows: the third-stage excavation (unacceptable); the fourth-stage excavation (poor); and the fifth-stage excavation (excellent).

Table 6. The predicted maximum displacements and corresponding level classifications for each stage of the excavation.

	Monitoring Value	**BPNN**			**MFLN**			**RIDO**		
	Max. Displacement (cm)	**Max. Predicted Displacement (cm)**	**Error (%)**	**Grade**	**Max. Predicted Displacement (cm)**	**Error (%)**	**Grade**	**Max. Predicted Displacement (cm)**	**Error (%)**	**Grade**
The 3rd-stage excavation	2.1	1.95	7.0%	Excellent	2.18	3.8%	Excellent	1.07	48.9%	Unqualified
The 4th-stage excavation	1.9	2.26	18.9%	Poor	2.08	9.2%	Excellent	1.68	11.3%	Poor
The 5th-stage excavation	2.34	2.02	13.5%	Poor	2.00	14.6%	Poor	2.53	8.0%	Excellent

Table 7 lists the results for the predicted maximum displacement occurrence locations and corresponding level classifications in each stage of the excavation. All three methods achieved good prediction results for the location of maximum wall displacement, with errors of less than 2 m above or below the surface of the completed excavation.

Table 7. The predicted maximum displacement occurrence locations and corresponding level classifications in each stage of the excavation.

	Monitoring Value	**BPNN**			**MFLN**			**RIDO**		
	Occurrence Location GL (m)	**Occurrence Location GL (m)**	**Error (%)**	**Grade**	**Occurrence Location GL (m)**	**Error (%)**	**Grade**	**Occurrence Location GL (m)**	**Error (%)**	**Grade**
The 3rd-stage excavation	−7.93	−6.93	1.00	Successful	−7.93	0.00	Successful	−8.60	0.67	Successful
The 4th-stage excavation	−11.43	−9.43	2.00	Successful	−9.43	2.00	Successful	−11.80	0.37	Successful
The 5th-stage excavation	−13.43	−13.93	0.50	Successful	−11.93	1.50	Successful	−13.88	0.45	Successful

3.4. Application of Prediction Model

The applicability of the proposed prediction model for excavation cases was assessed using a case study, which is the Yongfengyu project located in Xinyi District, Taipei, Taiwan. This study also compared the results of the prediction model with those of the inverse analysis obtained by Chen and Ji [45] using RIDO 3.07 version.

In this project, the excavation depth for the foundation was 12.25 m; the wall depth was 21.5 m, and the wall thickness was 60 cm. The excavation was divided into five stages. Based on previous reports on geological analysis, construction procedures, and monitoring data, the compilation of input variables resulted in 57 data points for validation.

The monitored vs. predicted displacements of different excavation stages are shown in Figure 8a–c, and the level statistics for each observation point in each excavation stage are summarized in Table 8. The performance of the MFLN was as follows: the third-stage excavation (47.4%; success); the fourth-stage excavation (63.2%; acceptable); and the fifth-stage excavation (89.5%; success). Overall, more than 70% of the cases presented low relative errors (i.e., below 40%), far exceeding the inverse analysis results obtained by using RIDO.

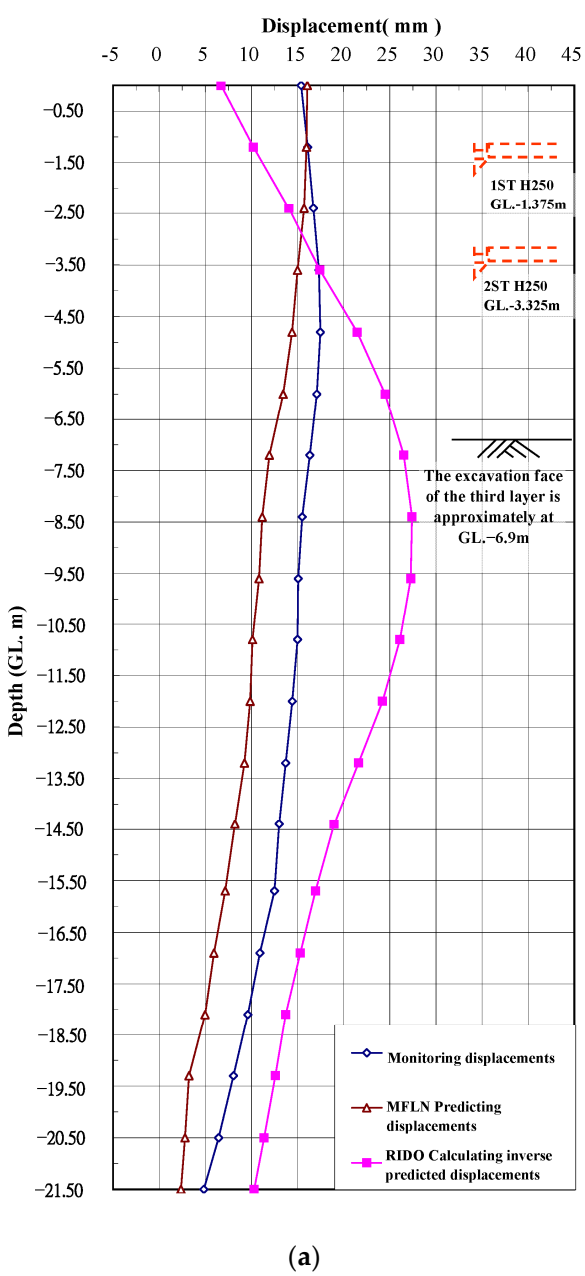

(**a**)

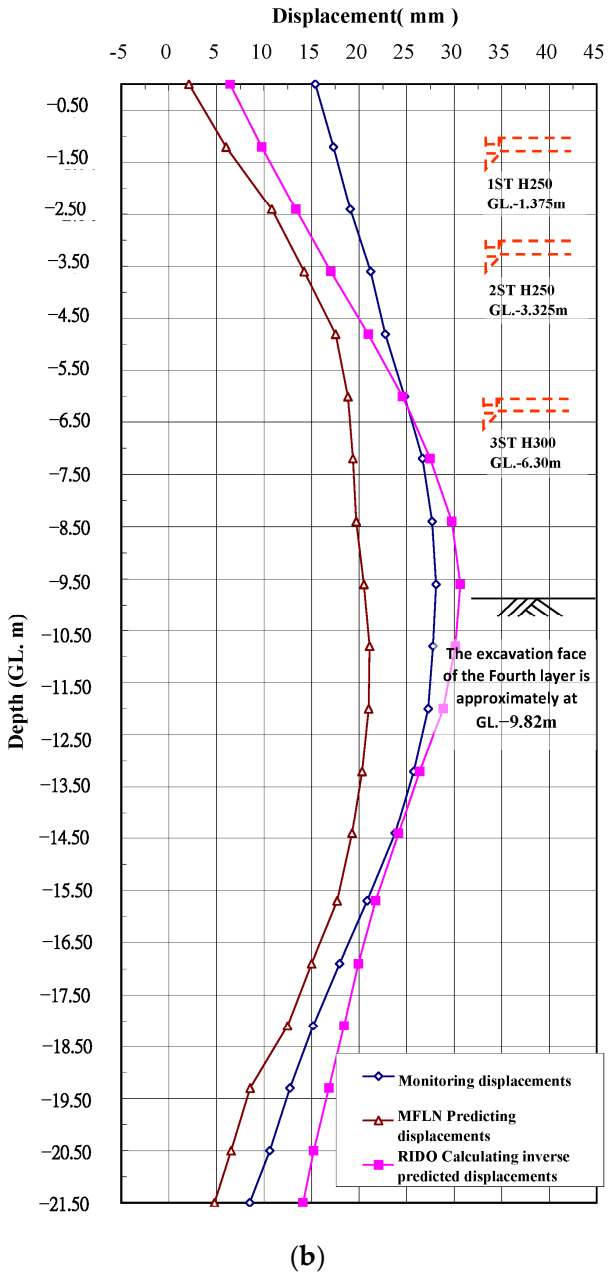

(**b**)

Figure 8. *Cont.*

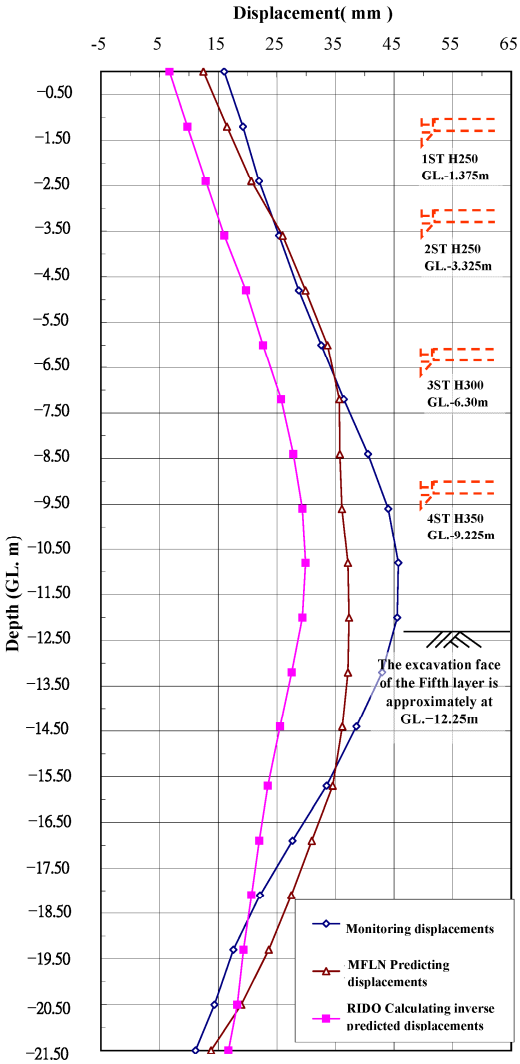

(**c**)

Figure 8. The monitoring and predicted displacements map for Yongfengyu project: (**a**) The 3rd-stage excavation; (**b**) The 4th-stage excavation; (**c**) The 5th-stage excavation.

Table 8. Statistics table of predicted excavation observation point levels.

Mode		MFLN			RIDO (Inverse Analysis Program)		
Grade \ Excavation Stage		The 3rd-Stage Excavation	The 4th-Stage Excavation	The 5th-Stage Excavation	The 3rd-Stage Excavation	The 4th-Stage Excavation	The 5th-Stage Excavation
Success (0~20%)	Number	5	4	14	2	12	3
	Proportion	26.3%	21.1%	73.7%	10.5%	63.2%	15.8%
Satisfactory (20~30%)	Number	4	8	3	1	2	3
	Proportion	21.1%	42.1%	15.8%	5.3%	10.5%	15.8%
Fair (30~40%)	Number	4	3	2	3	1	9
	Proportion	21.1%	15.8%	10.5%	15.8%	5.3%	47.4%
Failure (40% and above)	Number	6	4	0	13	4	4
	Proportion	31.6%	21.1%	0.0%	68.4%	21.1%	21.1%

Table 9 lists the predicted maximum displacements and the corresponding level classifications for each stage of excavation. The performance of the MFLN was as follows: the third-stage excavation (<10%; excellent); the fourth-stage excavation (24.9%; unacceptable);

and the fifth-stage excavation (18.4%; poor). Nonetheless, the overall errors were below 30%, far exceeding the inverse analysis results obtained using RIDO.

Table 9. Statistics table of relative error and level for maximum displacement and location.

Method	Actual Monitoring Value		MFLN					
Item	Max. Displacement (cm)	Occurrence Location (m)	Max. Predicted Displacement (cm)	Error (%)	Grade	Occurrence Location GL(m)	Error (m)	Grade
The 3rd-Stage Excavation	1.75	−4.8	1.60	8.1%	Excellent	−1.20	3.60	Satisfactory
The 4th-Stage Excavation	2.81	−9.6	2.11	24.9%	Unqualified	−10.80	1.20	Successful
The 5th-Stage Excavation	4.57	−10.8	3.73	18.4%	Poor	−12.00	1.20	Successful
Method			**RIDO (Inverse analysis program)**					
	Item		**Max. Predicted Displacement (cm)**	**Error (%)**	**Grade**	**Occurrence Location GL(m)**	**Error (m)**	**Grade**
	The 3rd-stage excavation		2.74	36.3%	Unqualified	−8.40	−3.60	Ok
	The 4th-stage excavation		3.07	8.4%	Excellent	−9.60	0.00	Successful
	The 5th-stage excavation		2.99	52.9%	Unqualified	−10.80	0.00	Successful

Table 9 also lists the predicted maximum displacement locations and the corresponding level classifications for each stage of excavation. The performance of MFLN was as follows: the third-stage excavation (2–4 m; successful); the fourth-stage and fifth-stage excavations (<2 m; successful). These results are comparable to the inverse analysis results obtained using RIDO. Overall, the MFLN network demonstrated good predictive capabilities.

4. Conclusions and Recommendations

4.1. Conclusions

From the above analysis results, the following conclusions can be drawn:

1. Twelve input variables were categorized into six network model combinations based on their attributes, characteristics, and interrelationships. In this study, model B-1 with 11 input variables was selected, and the prediction accuracy could be improved by including more input variables that corresponded to the output variable;
2. In the prediction of displacement for each observation point, the multilayer functional-link network (MFLN) prediction model achieved a success rate of 70%, while the back-propagation neural network (BPNN) prediction achieved only 61%. This demonstrates that utilizing the enhanced type of neural network for predicting wall displacement can yield superior outcomes;
3. In the prediction of the maximum wall displacement in each stage of the excavation, the MFLN prediction model outperformed the others, boosting an average prediction error of 9.2%. This was notably lower than the 13.1% error rate of the BPNN and significantly better than the 22.7% error rate of RIDO (a specific model or method, assuming an acronym based on your context). Overall, the application of MFLN resulted in at least a 5% enhancement in prediction accuracy. This underscores the efficacy of the MFLN network in augmenting the precision of predictions;
4. Based on the case study results, approximately 40.4% of the observation points were predicted to belong to the "successful" category, while around 26.3% were categorized as "acceptable". The combined percentage for these two categories amounts to nearly 66.7%. In contrast, the RIDO program's prediction for the combined percentage was only 40.4%. Therefore, the neural network-based wall displacement prediction system developed in this study demonstrates a high level of predictive accuracy when applied to the Taipei Basin area;

5. The retaining wall displacement prediction developed in this study is primarily applicable to the geological conditions of the Taipei Basin area, utilizing the top–down construction method with the diaphragm wall structures. Nevertheless, for regions with different geological conditions and construction methods, the proposed network can be adapted. It can be trained and tested using local case data, following the network establishment procedures outlined in this study. Upon verification, the adapted model can then be employed for predictive operations, extending the utility of our initial model beyond its original context and ensuring its adaptability and relevance in a variety of scenarios;
6. Through our research process, we discovered a correlation between the prediction accuracy of the network and the number of training cases used during the model establishment. The prediction error diminishes as the number of valid case studies increases. In practical applications, we anticipate enhanced completeness and applicability of the optimally constructed prediction network system by continuously incorporating additional engineering cases. Real-world monitoring data can serve as training examples, contributing to the iterative retraining of the prediction network. This ongoing refinement process, integrating new data and learning from them, is expected to fine-tune the system's performance, aligning it closely with the earlier assertion that prediction accuracy is correlated to the volume of training cases.

4.2. Recommendations

1. The results of input variable selection in the MFLN indicate a higher number of input variables corresponding to output variables, contributing to improved prediction accuracy. In the sensitivity analysis of test results, $NL2$ exhibited the highest sensitivity, with $NL1$ being the lowest. The marginal difference of approximately 0.63 between the high and low values demonstrates that all variable items impact the network's prediction accuracy. By incorporating additional input variable items, such as changes in support tonnage and groundwater level—which are easily obtainable monitoring data—the network's predictive accuracy should be enhanced;
2. This study revealed a correlation between network prediction accuracy and the volume of training cases used in model establishment. As the number of effective case volumes increases, the prediction error of the established forecasting system diminishes. Future applications can benefit from the continuous inclusion of engineering cases, utilizing actual monitoring data as training examples and feeding it back for network retraining. This iterative process is expected to enhance the comprehensiveness and applicability of the optimally constructed predictive network system. While the current MFLN displacement prediction is primarily targeted at the Taipei Basin area and adopts the top–down construction method, other regions can adapt local case data, follow the network establishment process outlined in this study for training and testing, and implement prediction tasks following a verification procedure.

Supplementary Materials: The following supporting information can be downloaded at https://www.mdpi.com/article/10.3390/sym15112093/s1, Table S1: Table of Deep Excavation Project Case Studies; Table S2: List of example data for network training and testing.

Author Contributions: Conceptualization C.-Y.W. and Y.-F.L.; methodology, C.-Y.W., C.-F.H. and Y.-F.L.; formal analysis, C.-Y.W.; investigation, C.-Y.W.; writing—original draft preparation, C.-Y.W. and C.-F.H.; writing—review and editing, C.-F.H.; funding acquisition, Y.-F.L. All authors have read and agreed to the published version of the manuscript.

Funding: This research was funded by "The Research Center of Energy Conservation for New Generation of Residential, Commercial, and Industrial Sectors" from the Ministry of Education in Taiwan under contract No. L7121101-19.

Data Availability Statement: The data are contained within the article and Supplementary Materials.

Conflicts of Interest: Author Chien-Yi Wu was employed by the Kenkul Corporation Company. The remaining authors declare that the research was conducted in the absence of any commercial or financial relationships that could be construed as a potential conflict of interest. The authors declare that this study received funding from the Ministry of Education in Taiwan under contract No. L7121101-19. The funder was not involved in the study design, collection, analysis, interpretation of data, the writing of this article or the decision to submit it for publication.

Appendix A

Table A1. Optimal network performance comparison table.

Network Architecture	BPNN		Network Architecture	MFLN		Network Performance Improvement Rate	
	Training	Testing		Training	Testing	Training	Testing
	RMS	RMS		RMS	RMS	Training	Testing
11-30-1	0.01272	0.01830	(11,11,11)-30-(1,1,1)	0.00449	0.01613	64.7%	11.9%
	0.01132	0.01946		0.00535	0.01930	52.7%	0.8%
	0.01181	0.02319		0.00449	0.01613	62.0%	30.4%
	0.01284	0.03033		0.00479	0.02136	62.7%	29.6%
	0.01284	0.02515		0.00542	0.02140	57.8%	14.9%

Table A2. List of optimal network configuration parameter values.

Item \ Mode	BPN	MFLN
Normal input processing units	11	11
Number of hidden units in the second layer of a normal neural network	30	30
Number of hidden units in the first layer of a normal neural network	0	0
Normal output processing units.	1	1
Number of units in the logarithmic input processing layer.	-	11
Number of units in the logarithmic output processing layer.	-	1
Number of units in the exponential input processing layer.	-	11
Number of units in the exponential output processing layer.	-	1
Number of learning cycles	3000	4000
Initial learning rate.	1.0	1.0
Initial inertia factor.	0.8	0.5

Table A3. Statistics table of monitoring points for the third-stage excavation.

Grade (Displacement Relative Error) / Network Mode		BPN	MFLN
Success (0~20%)	Number	33	38
	Proportion	58.9%	67.9%
Satisfactory (20~30%)	Number	2	4
	Proportion	3.6%	7.1%
Fair (30~40%)	Number	2	1
	Proportion	3.6%	1.8%
Failure (40% and above)	Number	19	13
	Proportion	33.9%	23.2%

Table A4. Statistics table of monitoring points for the fourth-stage excavation.

Grade (Displacement Relative Error) / Network Mode		BPN	MFLN
Success (0~20%)	Number	24	29
	Proportion	42.9%	51.8%
Satisfactory (20~30%)	Number	10	5
	Proportion	17.9%	8.9%
Fair (30~40%)	Number	6	5
	Proportion	10.7%	8.9%
Failure (40% and above)	Number	16	17
	Proportion	28.6%	30.4%

Table A5. Statistics table of monitoring points for the fifth-stage excavation.

Grade (Displacement Relative Error) / Network Mode		BPN	MFLN
Success (0~20%)	Number	46	51
	Proportion	82.1%	91.1%
Satisfactory (20~30%)	Number	3	1
	Proportion	5.4%	1.8%
Fair (30~40%)	Number	3	1
	Proportion	5.4%	1.8%
Failure (40% and above)	Number	4	3
	Proportion	7.1%	5.4%

Appendix B

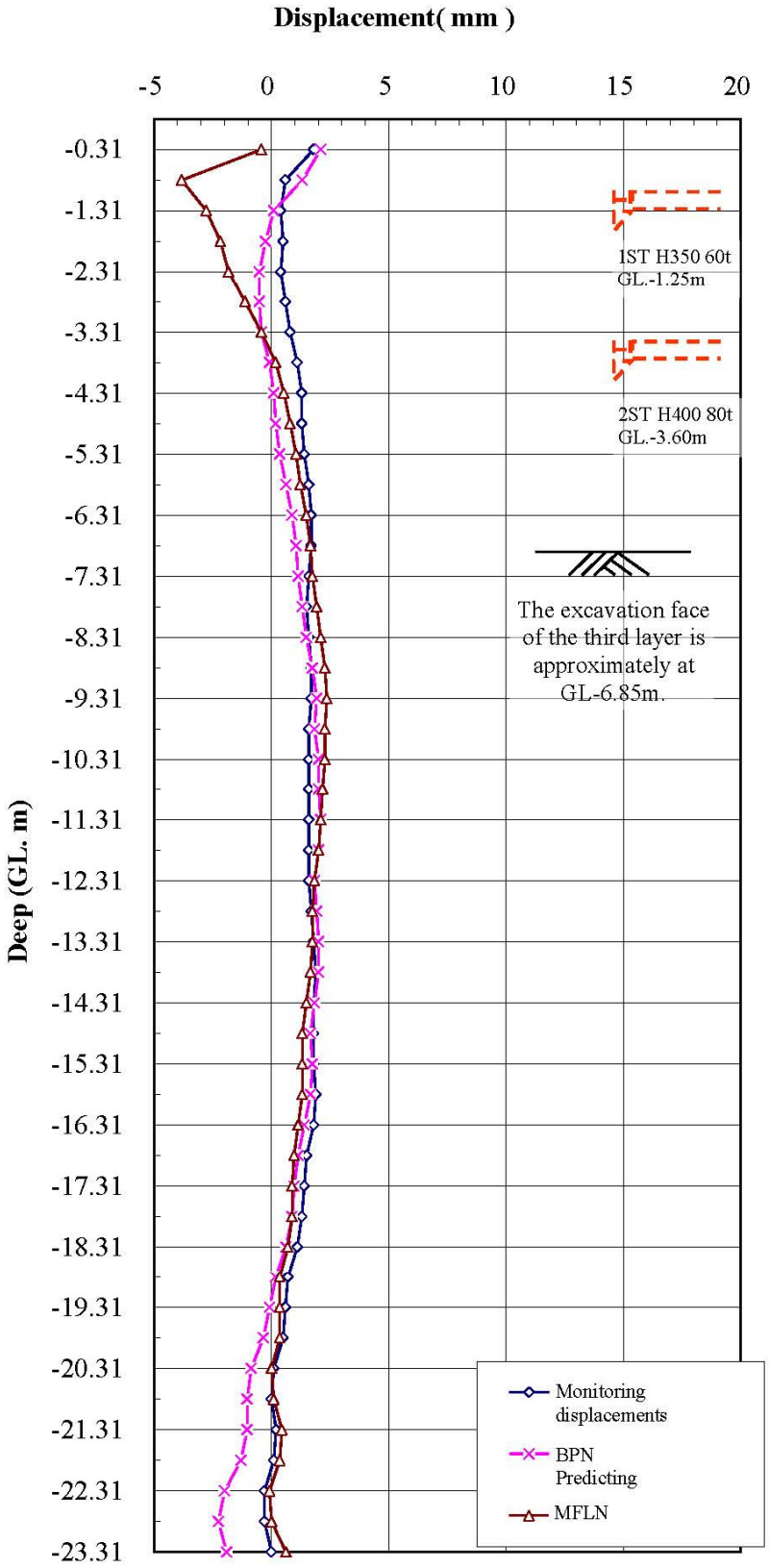

Figure A1. The prediction and monitoring displacements at the 3rd-stage excavation—case 10.

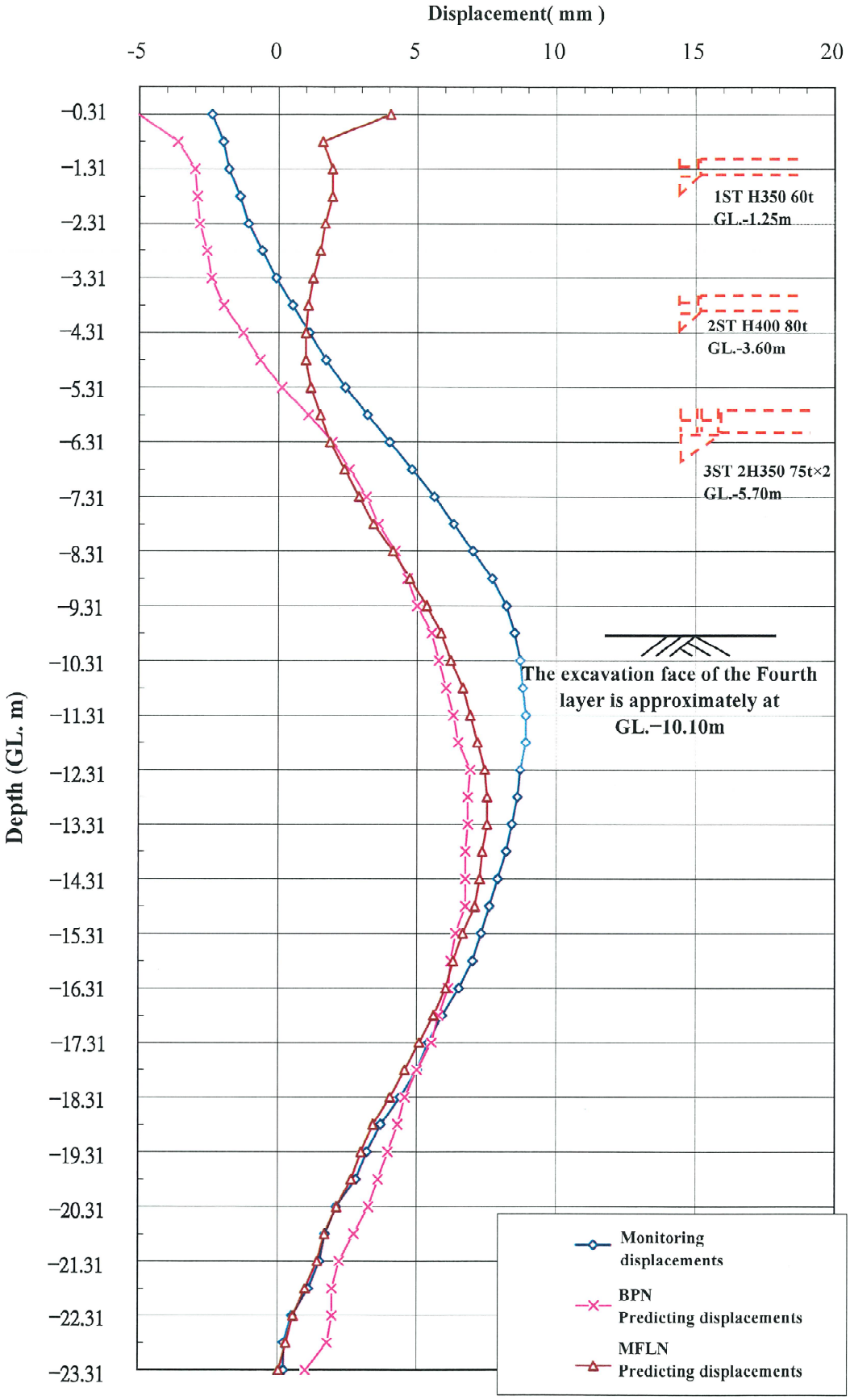

Figure A2. The prediction and monitoring displacements at the 4th-stage excavation—case 10.

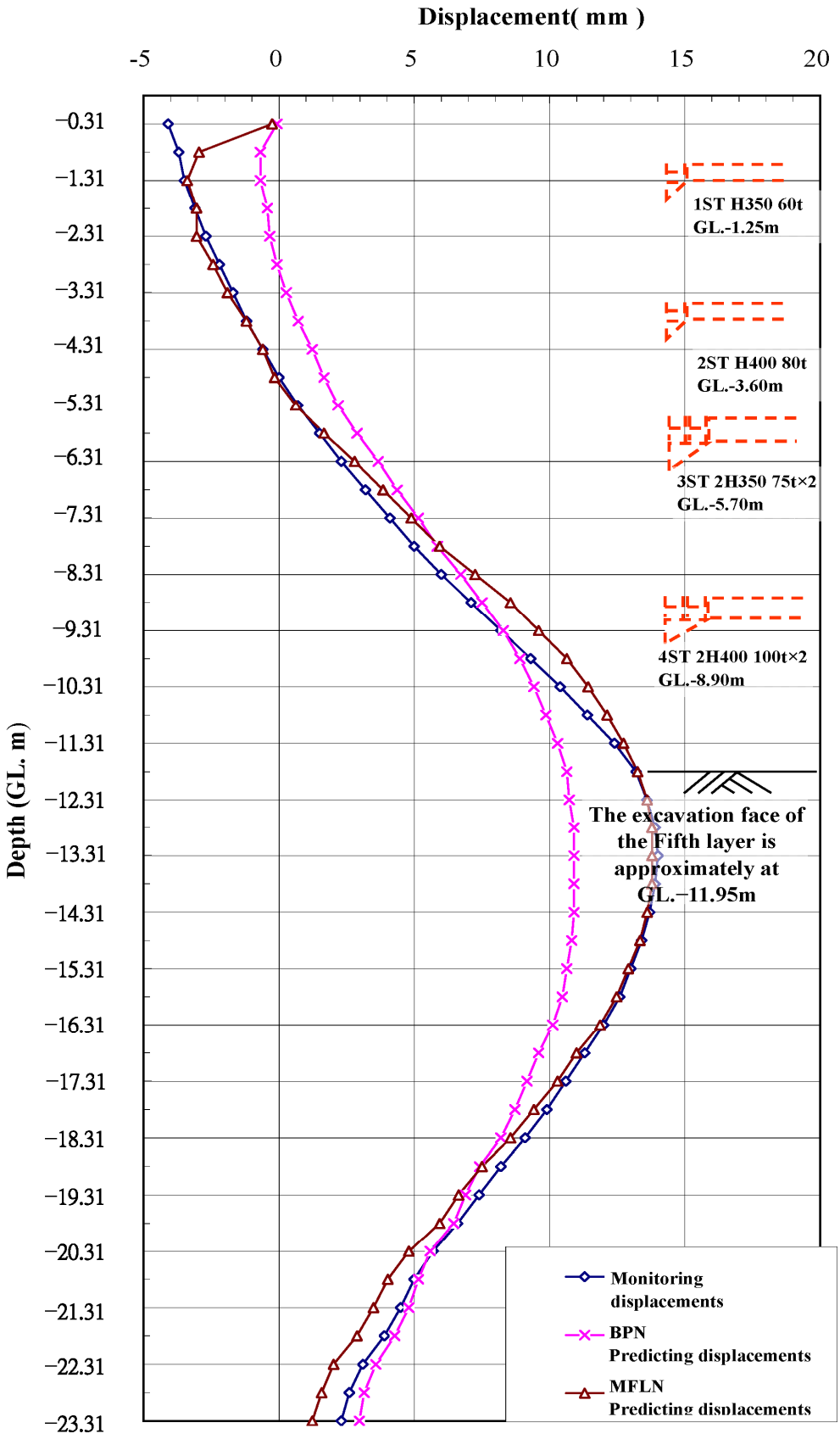

Figure A3. Prediction and monitoring displacements at the 5th-stage excavation—case 10.

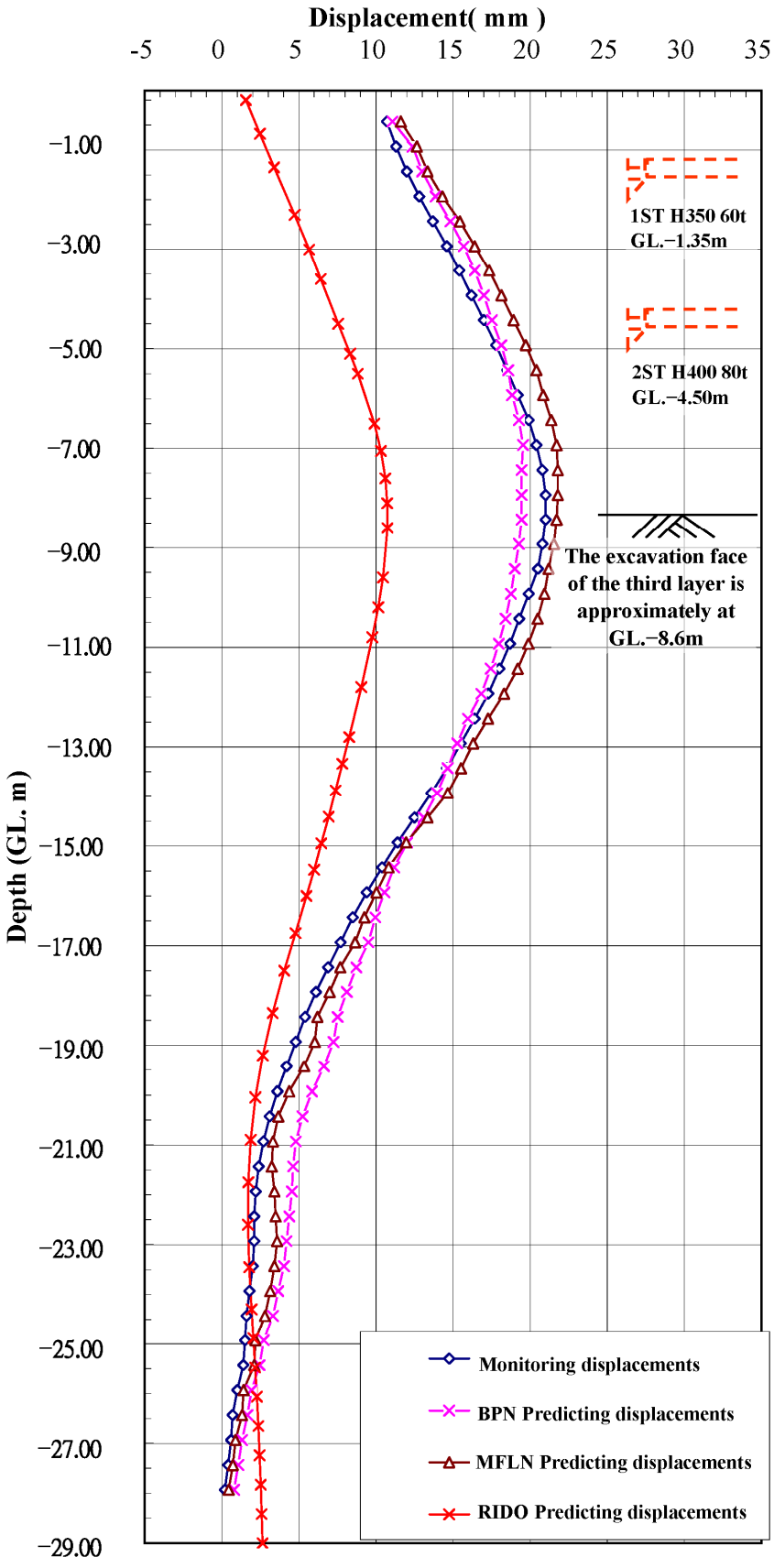

Figure A4. Prediction and monitoring displacements at the 3rd-stage excavation—case 10.

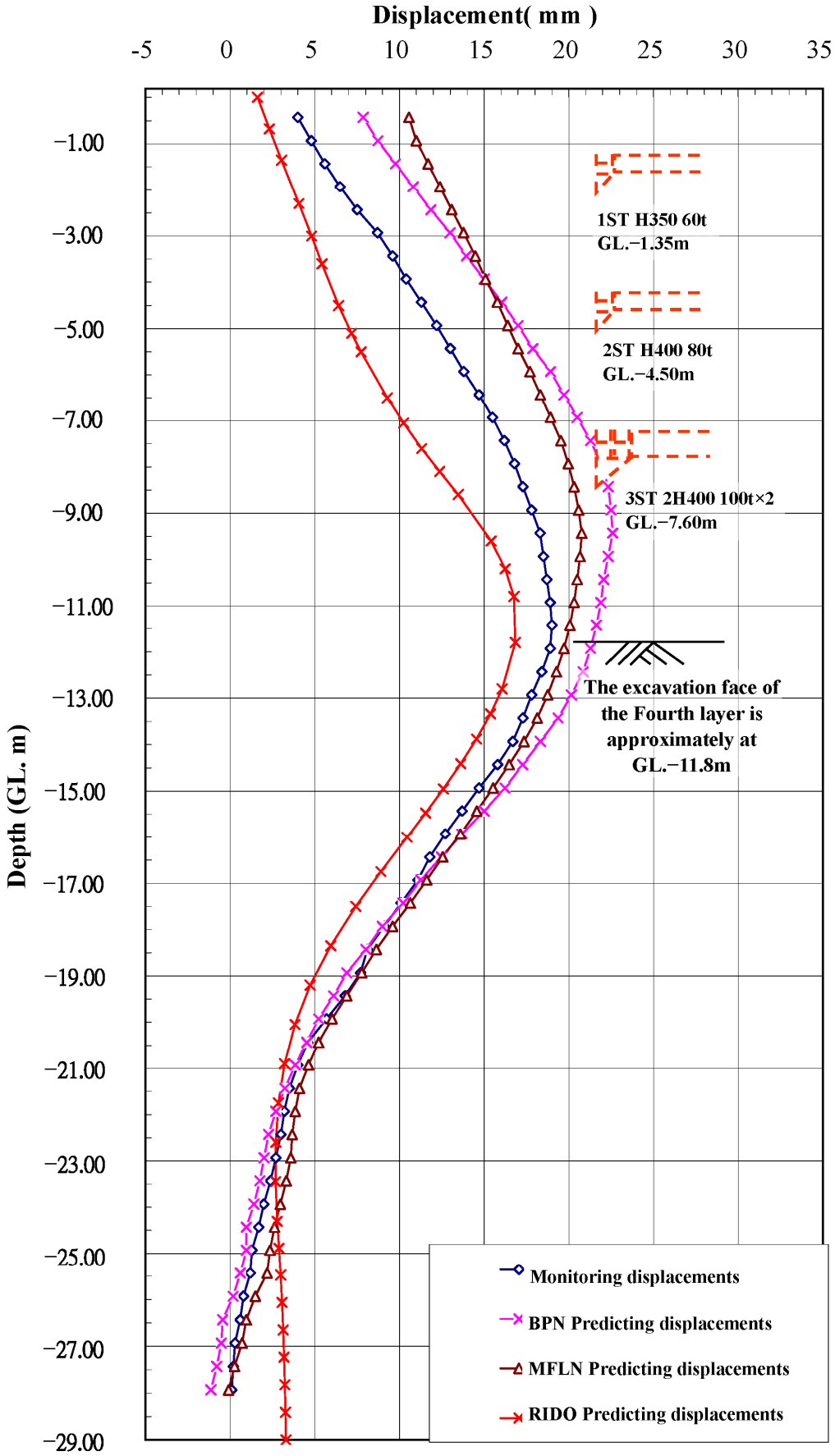

Figure A5. The prediction and monitoring displacements at the 4th-stage excavation—case 15.

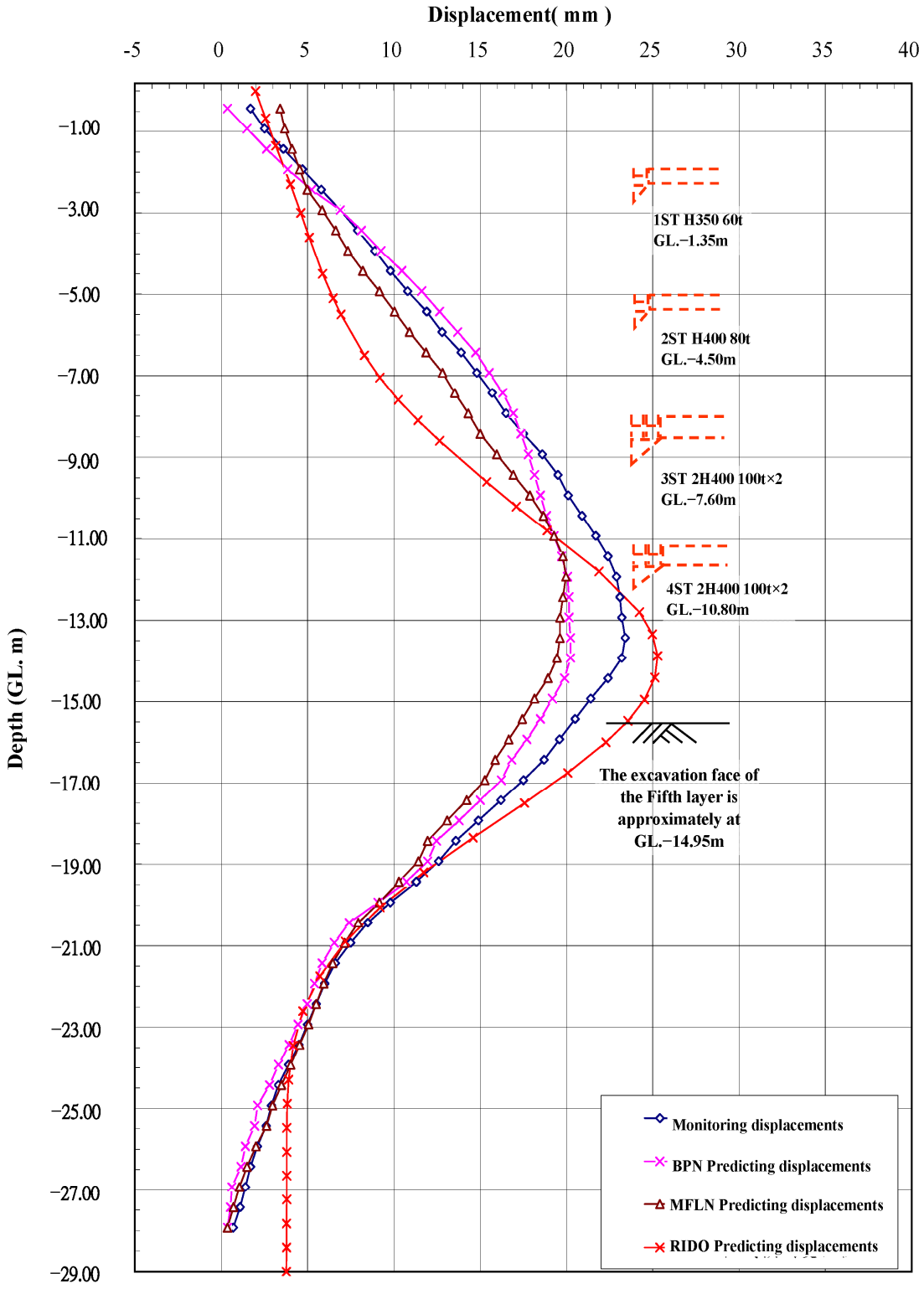

Figure A6. The prediction and monitoring displacements at the 5th-stage excavation—case 15.

References

1. Palmer, J.H.L.; Kenney, T.C. Analytical Study of a Braced Excavation in weak Clay. *Can. Geotech. J.* **1972**, *9*, 145–164. [CrossRef]
2. Mana, A.I.; Clough, G.W. Prediction of Movement for Braced Cut in Clay. *J. Geotech. Div. ASCE* **1981**, *107*, 756–777. [CrossRef]
3. O'Rourke, T.D. Ground Movement Caused by Braced Excavations. *J. Geotech. Div. ASCE* **1981**, *107*, 1159–1177. [CrossRef]
4. Chen, H.M. Ground Movements Caused by Deep Excavation. *Geotech. Technol.* **1987**, *20*, 19–33.
5. Wong, K.S.; Broms, B.B. Lateral Wall Deflections of Braced Excavation in Clay. *J. Geotech. Eng.* **1989**, *115*, 853–870. [CrossRef]

6. Clough, G.W.; O'Rourke, T.D. Construction Induced Movement of Institute Walls, Proceedings, Design and Performance of Earth Retaining Structures, ASCE. In Proceedings of the 1990 Specialty Conference on Design and Performance of Earth-Retaining Structures, Ithaca, NY, USA, 18–21 June 1990; pp. 439–470.
7. Hu, S.M. Design and Construction of Adjacent Property Protection for Deep Excavation Projects (Part 1). *Geotech. Technol.* **1992**, *40*, 35–50.
8. Lin, J.L.; Lee, J.Z. Study and Analysis of Ground Deformation in Deep Excavation. *Chin. Technol.* **1993**, *2*, 83–94.
9. Masuda, T.; Einstein, H.H.; Mitachi, T. Prediction of Lateral Deflection of Diaphragm Wall in Deep Excavation, Journal of Geotechnical Engineering. *Proceeding Jpn. Soc. Civ. Eng.* **1994**, *505*, 19–29.
10. Lao, C.M.; Zheng, Y. *Countermeasures for Hypothetical Engineering Problems*; Zhan Publishing: Beijing, China, 1998.
11. Lee, W.X.; Ni, Z.K.; Chen, Y.J. *Research on the Definition of Disaster-Prone Area Boundaries in Construction Foundation Engineering*; Institute of Architecture, Ministry of the Interior: New Taipei City, Taiwan, 2000; pp. 140–147.
12. Ou, Z.Y. *Theory and Practice of Analysis and Design for Deep Excavation Engineering*; Science and Technology Publishing Co., Ltd.: Beijing, China, 2002.
13. Goh, A.T.C.; Zhang, F.; Zhang, W.; Zhang, Y.; Liu, H. A simple estimation model for 3D braced excavation wall deflection. *Comput. Geotech.* **2017**, *83*, 106–113. [CrossRef]
14. Zhang, W.G.; Zhang, R.H.; Wu, C.Z.; Goh, A.T.C.; Wang, L. Assessment of basal heave stability for braced excavations in anisotropic clay using extreme gradient boosting and random forest regression. *Undergr. Space* **2020**, *7*, 233–241. [CrossRef]
15. Zhang, W.; Li, H.; Li, Y.; Liu, H.; Chen, Y.; Ding, X. Application of deep learning algorithms in geotechnical engineering: A short critical review. *Artif. Intell. Rev.* **2021**, *54*, 5633–5673. [CrossRef]
16. Lin, Y.C. Application of Evolutionary Fuzzy Neural Networks in Prediction of Deep Excavation Wall Deformation. Master's Thesis, Department of Construction Engineering, National Taiwan University of Science and Technology, Taipei City, Taiwan, 2004.
17. Hsieh, P.G.; Qu, C.Y. Shape of Ground Surface Settlement Profiles Caused by Excavation. *Can. Geotech. J.* **1998**, *35*, 1004–1017. [CrossRef]
18. Ou, C.Y.; Hsieh, P.G.; Chiou, D.C. Characteristics of ground surface settlement during excavation. *Can. Geotech. J.* **1993**, *30*, 758–767. [CrossRef]
19. Wu, P.Z.; Wang, M.J.; Peng, Y.R. Discussion on deformation of diaphragm wall. In Proceedings of the 7th Conference on Current Researches in Geotechnical Engineering, Taipei, Taiwan, 1997; pp. 601–608.
20. Woo, S.M.; Moh, Z.C. Geotechnical Characteristics of Soils in the Taipei Basin. In Proceedings of the 10th Southeast Asian Geotechnical Conference, Taipei, Taiwan, 16–20 April 1990; Volume 2, pp. 51–65.
21. Xu, Q.; Li, D. Geology and adjacent excavation settlement characteristics of the Kaohsiung MRT Red-Orange Line. In Proceedings of the Metro Construction and Underpinning Engineering Conference, 1997; pp. 113–116.
22. Zhang, J. Study on Surface Settlement Characteristics Induced by Deep Excavation and Its Prediction Model. Master's Thesis, National Cheng Kung University, Tainan, Taiwan, 2000.
23. Li, Y. Application of Neural Networks in Geotechnical Engineering. Master's Thesis, National Taiwan Ocean University, Keelung, Taiwan, 2005.
24. Chen, S.H. Numerical Analysis of Deep Excavation in Taipei City. Master's Thesis, National Taiwan University, Taipei, Taiwan, 1992.
25. Ou, J.; Shi, Q.; Xie, X. Practical considerations in design and analysis of diaphragm walls. *Geotech. Technol.* **1988**, *21*, 10–17.
26. Huang, C. Prediction of Deformation of Reverse Construction Deep Excavation Retaining Walls Using Artificial Neural Networks. Master's Thesis, National Taiwan Ocean University, Keelung, Taiwan, 2002.
27. Ji, S.; Chen, J.; Wang, J. Investigation of optimal soil parameters using the RIDO program. *Geotech. Technol.* **1999**, *75*, 61–67.
28. Li, W. Analysis of Deformation of Retaining Walls Induced by Deep Excavation Using a Single Strut Model. Master's Thesis, National Taiwan University, Taipei, Taiwan, 2000.
29. Lai, Q.; Yu, M. *Design and Construction Practice of Deep Excavation Engineering*; Chung-Wu Publishing: Hong Kong, China, 2001; pp. 94–112.
30. Wang, W. Study on the Analysis of Kaohsiung Deep Excavation Cases Using the RIDO Program. Master's Thesis, Cheng Shiu University, Kaohsiung, Taiwan, 2010.
31. Liao, Y. Evaluation and Application of Limited Soil Analysis Models for Deep Excavation. Master's Thesis, National Taiwan University, Taipei, Taiwan, 2011.
32. Zhang, J. Application of Neural Networks in Civil Engineering. Master's Thesis, National Central University, Taoyuan, Taiwan, 1993.
33. Ji, S.; Chen, J.; Zhan, J. Application of neural networks in predicting deformation of deep excavation retaining walls. *Geotech. Technol.* **2002**, *91*, 55–64.
34. Li, W. Prediction of Deformation of Deep Excavation Retaining Walls—Application of Evolutionary Support Vector Machine Inference Model (ESIM). Master's Thesis, National Taiwan University, Taipei, Taiwan, 2008.
35. Wu, J.; Chen, S. Prediction of deep excavation wall displacement using multi-layer function link networks. *J. China Civ. Eng. Water Conserv.* **2012**, *24*, 1–13.
36. Gioda, G.; Sakurai, S. Back-Analysis Procedure for the Interpretation of Field Measurements in Geomechanics. *Int. J. Numer. Analyt. Methods Geomech.* **1987**, *11*, 555–583. [CrossRef]

37. Whittle, A.J.; Hashash, Y.M.A.; Whitman, R.V. Analysis of Deep Excavation in Boston. *J. Geotech. Eng.* **1993**, *119*, 69–90. [CrossRef]
38. Ou, C.Y.; Tang, Y.G. Soil Parameter Determination for Deep Excavation Analysis by Nonlinear Optimization. *J. Chin. Inst. Eng.* **1994**, *17*, 671–688. [CrossRef]
39. Chi, S.Y.; Chern, J.C.; Wang, C.C. Information Construction Approach for Deep Excavation. In Proceedings of the International Symposium of Geotechnical Aspects of Underground Construction in Soft Ground, Tokyo, Japan, 19 July 1999; Balkema: Rotterdam, The Netherlands, 1999; pp. 471–476.
40. Tang, Y.G.; Kung, T.C. Application of nonlinear optimigation technigue to back analyses of deep excavation. *Comput. Geotech.* **2009**, *36*, 276–290. [CrossRef]
41. Jan, J.C.; Hung, S.L.; Chi, S.Y.; Chern, J.C. Neural Network Forecast Model in Deep Excavation. *J. Comp. Civ. Eng.* **2002**, *16*, 59–65. [CrossRef]
42. Chern, S.G.; Tsai, J.H.; Chien, L.K.; Huang, C.Y. Predicting Lateral Wall Deflection in Top-down Excavation by Neural Network. *Int. J. Offshore Polar Eng.* **2009**, *19*, 151–157.
43. Yicheng, Y. *Application and Implementation of Neural Network Models*; Ru Lin Publishing Company: Taipei, Taiwan, 2003.
44. Wu, J.Y.; Chen, C.J. Application of Multilayer Function Link Network in Predicting Deep Excavation Wall Deformation. *J. Chin. Civ. Eng.* **2012**, *24*, 1–13.
45. Jinqing, C.; Shuyong, J. *Collection of Deep Excavation Case Data in the Taipei Basin and Feedback Analysis of Parameters*; Chung Hsing Engineering Consultants Foundation: Taipei, Taiwan, 1999.